

ARIEL M2M ACTUATOR DERISKING

Aiala Artiagoitia⁽¹⁾, Carlos Compostizo⁽¹⁾, Paolo Zaltron⁽²⁾, Jameson Barlow⁽³⁾, Mike Anderson⁽⁴⁾

⁽¹⁾ SENER, Av. Zugazarte 56, 48930 Las Arenas (Bizkaia) Spain, Email: aiala.artiagoitia@aeroespacial.sener

⁽²⁾ ESA/ESTEC, Keplerlaan 1, Postbus 299, 2200 AG, Noordwijk, NL, Email: paolo.zaltron@esa.int

⁽³⁾ CDA Intercorp, 450 Goolsby Blvd., Deerfield Beach Fl, 33442, Email: jbarlow@cda-intercorp.com

⁽⁴⁾ ESTL, ESR Technology, 202 Cavendish Place, Birchwood Park, WA3 6WU, (UK), Email: mike.anderson@esrtechnology.com

ABSTRACT

The Atmospheric Remote-sensing Infrared Exoplanet Large-survey (ARIEL) mission has the aims to move forward the understanding of exo-planetary science, by which we mean understanding the nature of the exo-planetary bodies and their formation and evolutionary history. For this reason, in March 2018, ESA selected ARIEL as the M4 mission, to be launched in 2028.

The focusing of the telescope will be done on the M2 mirror which is mounted a focussing and orientation mechanism (M2M). The M2M will be composed of three linear actuators, which provide the desired three degrees of freedom motion.

This de-risking activity consists in the development of the ARIEL Mirror Mechanism (M2M) cryogenic actuator including its design, manufacturing and qualification testing.

1. INTRODUCTION

The M2M is the link between the optical bench and the secondary mirror and shall provide capability to adjust it in three dof, one translation and two rotations. The M2M shall also maintain the position of the M2 mirror from the position defined during telescope alignment on ground, launch and in orbit transfer environment without any hold down device.

The M2M is composed of three linear actuators, which provide the desired three degrees of motion. The displacement in Z is obtained with the three actuators acting at same time. The two rotations are obtained by a differential linear displacement of the three actuators, which are placed in a triangular symmetrical arrangement.

The joint between fixed interface (I/F) and tray and M2 mirror and tray is based on flexible elements.

The actuators and most of the parts have to be made of Ti6Al4V. However, the interface parts (Support I/F Structure and the Mirror I/F Plate) are to be made in Aluminium to be compatible with the mirror and telescope structure.

The M2M is based on the actuators and mechanisms developed for the GAIA and EUCLID missions.

The main objectives of the activity described in this paper are:

- A trade off to confirm the Gaia and Euclid M2M assembly concept can be translated to ARIEL M2M
- Required design modifications
- Manufacturing of one actuator
- Complete test verification of one actuator in relevant environment including its life
- M2M Mechanism assembly baseline design

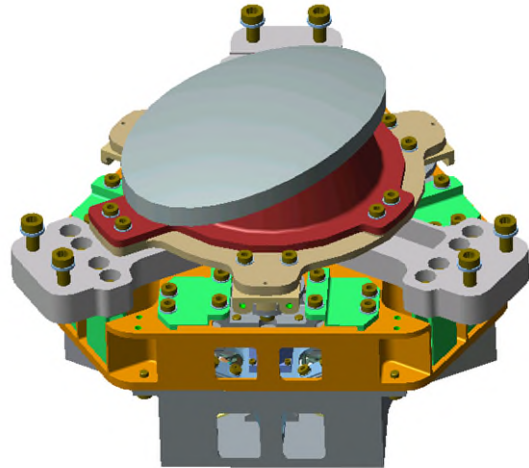


Figure 1 ARIEL M2MM configuration

2. DESIGN REQUIREMENTS

Main requirements of the mechanism:

- Overall stroke $\pm 350 \mu\text{m}$
- Resolution shall be better than $0.1 \mu\text{m}$
- Accuracy shall be kept below $\pm 2 \mu\text{m}$
- Full performances to be demonstrated at 40K
- Fulfil required lifetime of 80 duty cycled at Customer plus Sener AIV additional cycles

3. EVOLUTION OF REQUIREMENTS AND PERFORMANCES

Next table collects main differences in GAIA, EUCLID and ARIEL performances.

	GAIA	EUCLID	ARIEL
M2 Mirror Mass	1.9 Kg	< 3.1 Kg	< 1.5 Kg
M2M mass/QS	< 5.0 Kg / 30g	< 3.5 Kg / 28g	< 8.0 Kg / 30g
D.o.f. control	5 axes	3 axes (Disp Z + Rot X/Y)	3 axes (Disp Z + Rot X/Y)
Mechanism Stroke (dis/rot)	+/- 275 μ m +/-2 mrad	+/- 200 μ m +/- 1.5 mrad	+/- 350 μ m +/-2 mrad
Actuator Resolution	<0.5 μ m / 2 μ rad	<0.1 μ m / <2.5 μ rad	<0.1 μ m / <2.4 μ rad
Temp. Operational range (Design Temp.)	110 K to 313 K	110 K to 313 K	40 K to 303 K
Volume (mm)	L 260 x W 110 x H 150	Hexagonal 214 x H 150	Hexagonal 214 x H 150
Positional Accuracy	< \pm 3 μ m < \pm 40 μ rad	+/- 3 μ m +/- 30 μ rad	+/- 2 μ m +/- 40 μ rad

Table 1 Comparison between GAIA, EUCLID and ARIEL performances

4. GENERAL ACTUATOR CONFIGURATION

The linear actuator is a mechanism that provides resolution better than 0.1 μ m over a travel of +/- 350 μ m with stable positions at any position of the stroke. It also has high load capability to withstand launch loads without losing the launch position.

The different components of the actuator are basically:

- A motor-reducer from CDA Intercorp, which includes a stepper motor and three stages gear reducer with a M3 thread spindle at output.
- A symmetrical flexible structure, which includes two levers, two flexural joints or pivots, the output interface providing a reduction ratio and the I/F to fix to the M2MM tray.
- A Vespel SP3 nut which joins the flexible structure via two blades to the spindle.
- Two end stops at the beginning and end of the stroke for nut and blades protection and zeroing.
- Two micro-switches one main and one redundant for turns counting.
- A support structure where the motor-reducer and the top support of the spindle are mounted.

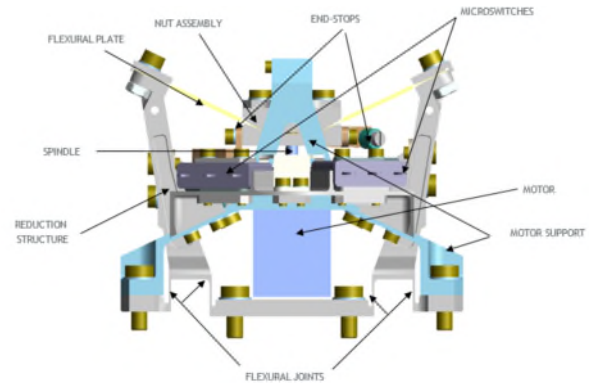


Figure 2 Actuator main parts

The design of the actuator for the ARIEL M2M:

- Range operational of +/-350 μ m with end stops at both extremes
- Resolution: equal to or better than 0.1 μ m
- Give stable positions with motor de-energized with a maximum external load of 441N
- High output axial stiffness
- Operational frequency: 54 Hz
- Operational temperature range from 40K to 303K.
- Non-Operational temperature range from 30K to 353K.
- Operational restrictions. The actuator is lubricated with MoS2 due to the low temperatures required.



Figure 3 ARIEL M2M Actuator

5. ACTUATOR TESTS

Actuator test campaign includes:

- Functional test at ambient (Including life cycles)
- Actuator vibration test
- Actuator TV test. Thermal cycling and functional test at 40K (Including life cycles)

The major effort during the test campaign was dedicated to the verification of functional performances verification at 40K. The final objective of the test was to demonstrate that the actuator was able to work at 40K.

Functional and Life Test at Ambient

The test set-up for the measurement of the output displacement of the actuators with capacitive sensors is shown in the following figure. The actuator must be operated in dry N2 environment (<5% HR).

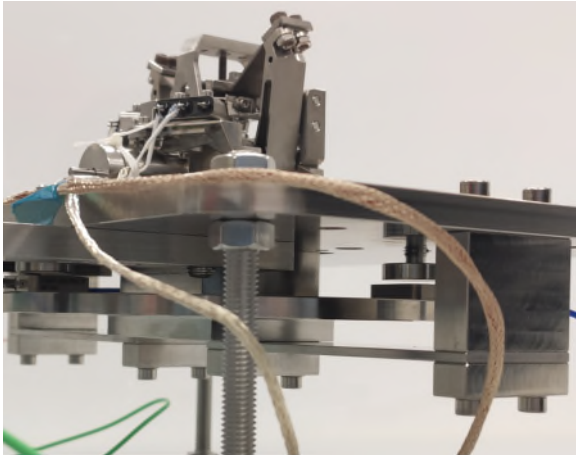


Figure 4 Test set-up for displacement measurement

Actuator motorization torque was verified via measurement of threshold current. It was checked that the actuator moved with 1/3 of the motor torque capabilities without losing steps.

The stroke between end stops is 749µm. The displacement of the output of the actuator was calculated as the mean value of three capacitive sensors.

The telemetry operated adequately: Microswitches were activated at every actuator turn (15 times).

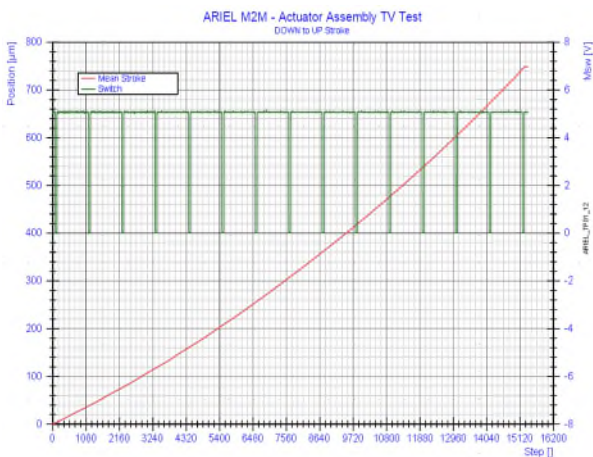


Figure 5 Stroke and telemetry verification

In addition, 444 cycles (556.643 motor turns) were done in N2 environment.

Vibration Tests

The main objective of the vibration test was the preconditioning of the actuator for continue with the life testing.

The first resonance frequency of the assembly was at 630 Hz.

Sine qualification level vibration loads were up to 28g in the frequency range of 25Hz to 35Hz and 5g at 140Hz.

Random qualification level was 10gRMS. The specified input was notched to 7.5gRMS in the fundamental global resonant frequencies, in order to limit the loads in the actuator.

The actuator was test assembled with the dummy of the M2 Mirror:

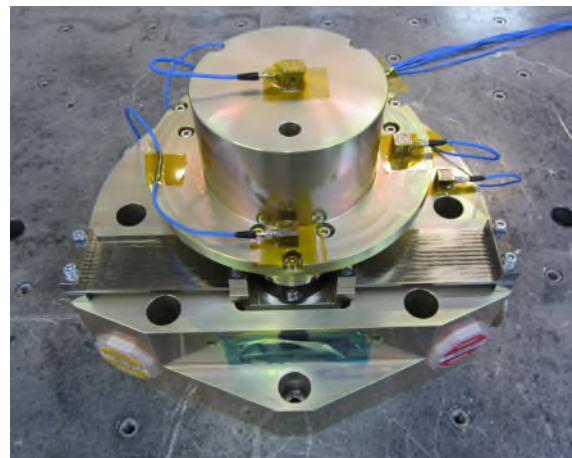


Figure 6 Stroke and telemetry verification

Thermal Vacuum and Life Test

The objective of test was to verify that the actuator was able to operate at 40K.

The test was carried out into the cryostat available at Sener premises. The set-up used for displacement measurement is the same than in functional test at ambient, however, only one capacitive sensor was connected to reduce the heat transmission to the equipment and ensure the target temperature is achieved.

Additionally, several copper braids were attached from the test article to the cryostat baseplate, including the braids of motor and microswitches harness.

The cryostat has thermal shields to isolate the equipment. Moreover, a MLI was installed between the equipment and thermal shields to increase the isolation.

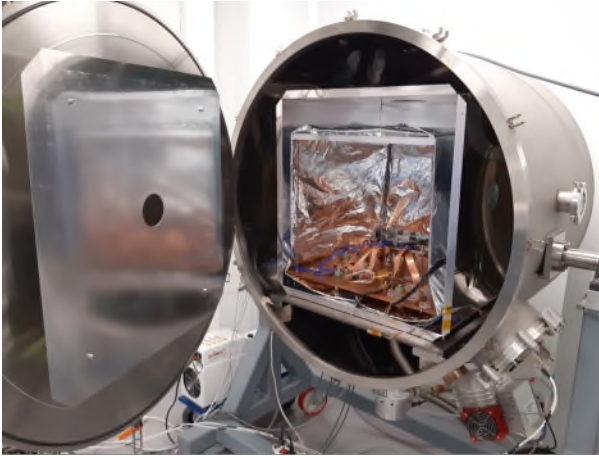


Figure 7 Cryostat overview

The test set-up for the measurement of the movements of the actuator with a capacitive sensor is shown in the following photograph.

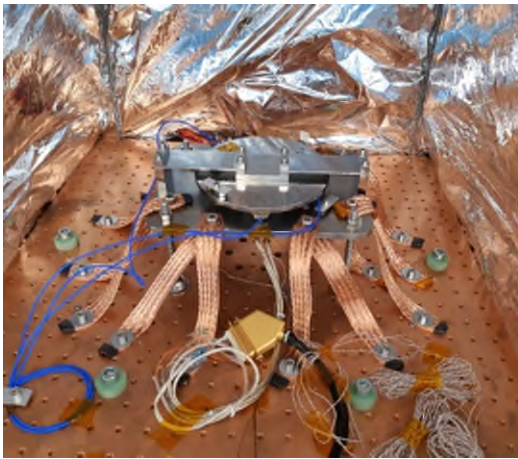


Figure 8 Test article and test set-up installed on cryostat baseplate

The following measurements were carried out at ambient temperature:

- Torque margin verification
- Stroke & Telemetry verification
- Life cycles: 76 operational cycles have been carried out at ambient during the initial tests at ambient, which is 1/4 of cycles at vacuum.

The following measurements were carried out at minimum operational temperature (40K):

- Torque margin verification
- Stroke & Telemetry verification

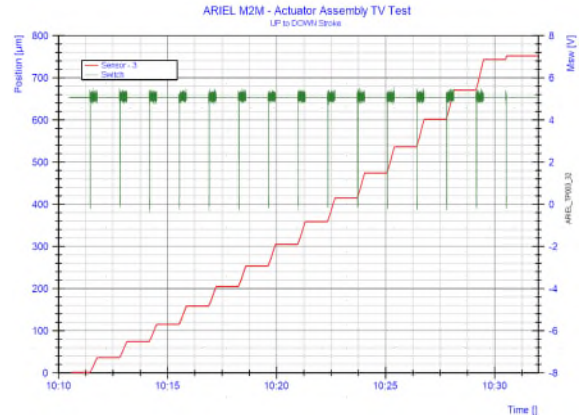


Figure 9 Stroke and Telemetry verification

Performances at 40K		Success Criteria
Operational Stroke [µm]	714	> 700
Maximum Error [µm]	1.75	< 2
Resolution [µm/step]	<0.067	< 0.1

Table 2 Actuator performances at 40K

- During life cycling a non-usual behaviour was detected in actuator displacement. In cycle number 50 (motor turn number 750.966) the operational stroke was not completed. After some additional movements, the actuator stopped.

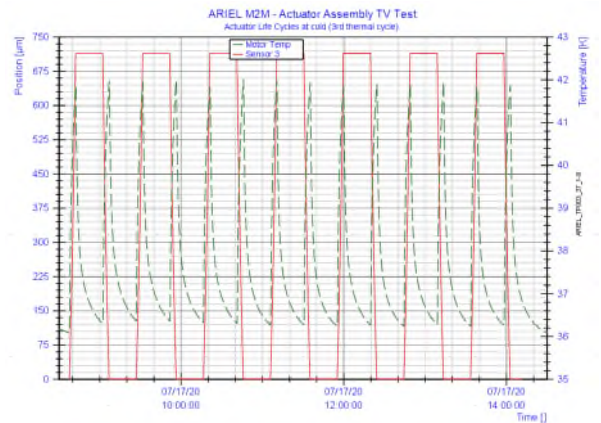


Figure 10 Actuator typical behaviour at 40K

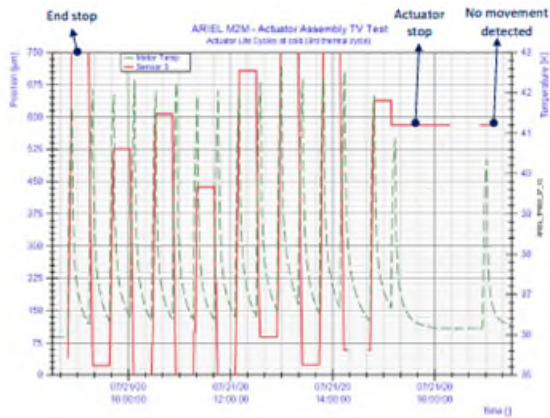


Figure 11 Actuator failure detection

6. ACTUATOR DISASSEMBLY

Spindle and Nut Inspection

The motor-reducer spindle and Vespel SP-3 nut were inspected with a microscope. As can be observed in following figures, some small particles of Vespel were found attached to the spindle and Vespel nut.

The Vespel nut wear is considered typical after such amount of cycles, and therefore, it is not the cause of the actuator failure.

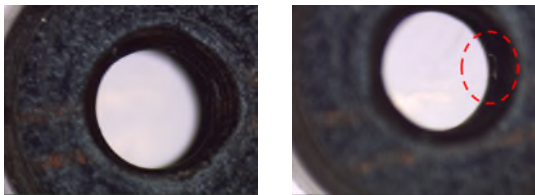


Figure 12 Nut inspection

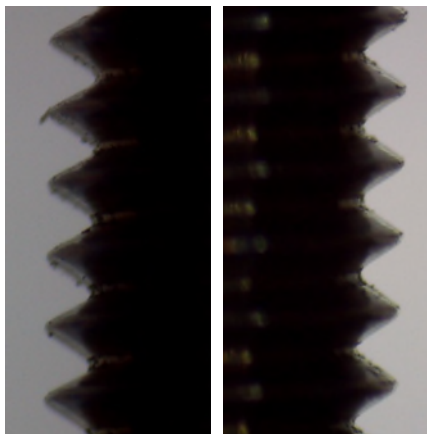


Figure 13 Spindle inspection

Motor-reducer inspection at CDA

The modules were separated from one another, and after the separation, each module was inspected.

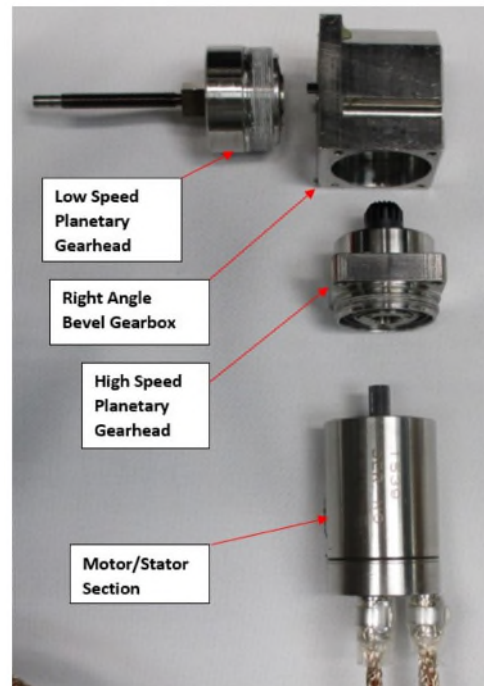


Figure 14 Motor and gearhead modules

- The Low Speed pinion output shaft was able to be fully backdriven by hand.
- The Right-Angle pinion was able to be fully backdriven by hand and found to rotate smoothly against the bevel gear within its gearbox.
- The high-speed gearhead was backdriven by hand but did not rotate smoothly. There were a couple of blocking/high spots detected during the initial rotation of the high-speed pinion, which prevented its full rotation by hand. However, during a subsequent check the pinion did rotate a full 360°, indicating that the blocking obstructions were freed.
- There was a visible wear band where the motor pinion meshes with the planet gears of the high-speed gearhead. The wear allowed the underlying base metal of pinion to become visible. Attempts were made to backdrive the motor rotor by hand, but it felt very crunchy and there were a couple of blocking/high spots detected which prevented its full rotation.

A large amount of brown debris was identified in and around the motor rotor's rear bearing. The debris was also found within the stator bore in the rear bearing's location after it was removed.



Figure 15 Motor bearings during disassembly

Upon removal of the rotor it was observed that the rear bearing could not spin freely while the front bearing could. During inspection of the bearings showed contact marks on the crest of the ribbon cage from possible interference with the races.

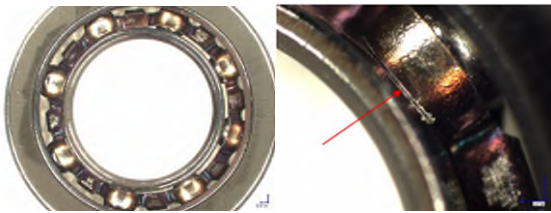


Figure 16 Rear motor bearing

The inspection was completed with the complete disassembly of each tribological components gears, ball bearings and planet pins.

Motor-reducer inspection at ESTL

The MoS₂ lubrication of the pieces was carried out by ESTL, and therefore, all the components were delivered to them for detailed inspection.

Rear Motor Bearing

The failed bearing was disassembled by firstly removing the cage and pushing the balls together so that the rings could be separated. More force than would normally be required was needed to push the balls together.

- Inner ring and Outer rings – there was no evidence of the MoS₂ lubricant on the raceway and metallic wear was observed.
- Inner ring -Marks consistent with metallic wear due to cage contact were present on both lands.
- Balls – the balls appeared dull and pitted, consistent with metallic wear.
- Cage – the edges of the cage appeared metallic wear with no MoS₂ remaining. Additionally, the MoS₂ was worn at each end of the ball pockets and the substrate exposed, although it should be noted that wear was not even in all ball pockets.

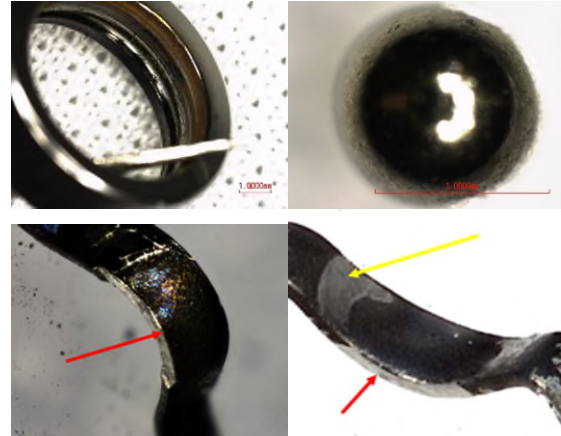


Figure 17 Rear motor bearing ring, ball and cage

Front Motor Bearing

This bearing was disassembled and examined optically for comparisons with the Rear Motor Rotor Bearing. This bearing was in better condition than the Rear Motor Rotor Bearing.

- Raceways – prior to disassembly the bearing rotated freely. Examination of the raceways revealed that MoS₂ was still present and it was also still present on the lands, although there were marks on the lands where the cage had been in contact.
- Cage – MoS₂ was still present in the ball pockets and light brown marks were evident where the ball had contacted the pockets.

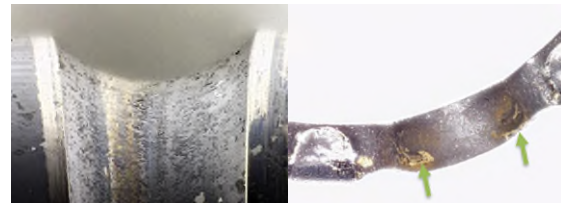


Figure 18 Front motor bearing ring and cage

Remaining ball bearings

Although emphasis was placed upon the Motor Rotor Bearings, all other bearings were inspected, although they were not so deeply examined.

SEM/EDAX of motor ball bearings

Following the optical examination, a SEM equipped with EDAX facilities was used to determine the nature of debris. The results from the rotor outer bearing inner ring raceway and lands are provided in the following Figures.

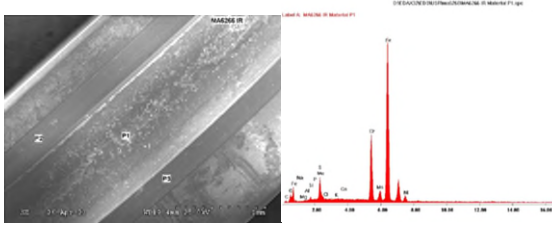


Figure 19 Rear Bearing Ring SEM/EDAX Analysis

Results showed that in addition to the Fe and Cr contained in 440C steel, Ni was also present in small quantities on the lands and a slightly larger peak was observed on the raceway. As Ni is not present in 440C of the bearings tracks, this element is therefore a contaminant and the most likely source is from the 300-series stainless steel cage. Note also, that some MoS₂ was detected and most probably originated from transferred debris or remnants still remaining. From the optical examination, no MoS₂ coating was visible on the raceway or parts of the lands identified by P1 and P2.

In addition, O-peaks were detected upon spectra from worn and unworn areas of the cage, but it was not possible to determine if this O-peak was from moisture or gaseous O combining with either the Fe or MoS₂ on the cage.

Following figure illustrates the surface of a typical ball and the EDAX spectrum confirms Ni present.

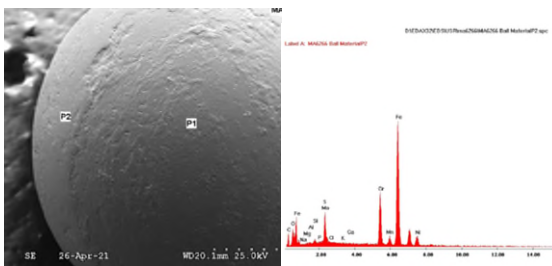


Figure 20 Rear Bearing Ball SEM/EDAX Analysis

The brown debris on the outer ring was analysed and the results show that Mo, S and O are present in addition to Fe and Cr. Note that there was not any Ni found. These spectra are more likely to indicate that the debris contains MoS₂ and not oxidised cage material.

However, oxidised Fe from the bearings cannot be ruled out. O-peaks were detected upon spectra from the debris, but it was not possible to determine if this O-peak was from moisture or gaseous O combining with either the Fe or MoS₂ on the cage.

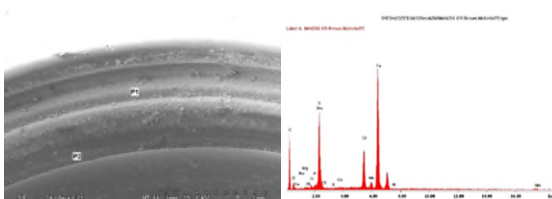


Figure 21 Brown debris from Rear Bearing outer ring

Gears

In general planet gears and pinions were in good conditions. The MoS₂ film was in good condition with light marks present.



Figure 22 Planet and Housing Gears

The Motor Rotor was inspected. The MoS₂ film on the teeth appeared intact, although some light marks consistent with contact with the opposing gear were evident.



Figure 23 Motor Rotor Pinion

Planet Pins

Wear of the MoS₂ is uneven and evident by the circumferential bands observed on all three pins. EDAX spectra exhibit strong Mo/S peak where they are not worn and a smaller peak in worn areas. Note that the pins were manufactured from WC and the presence of W was apparent in the EDAX spectra.



Figure 24 Low Speed Planet Pins

7. CONCLUSIONS

The actuator was able to operate at 40K. In fact, the actuator moved with 1/3 of the motor torque capabilities without losing steps at 40K.

The actuator operation was nominal until failure in life cycle number 599, which corresponds to 750.966 motor turns.

For investigation of the reasons of the failure of the actuator, it was decided to dismount the actuator and motor-reducer.

The investigation carried out to actuator pieces (Vespel nut and motor-reducer spindle) showed a typical

behaviour. For that reason, the investigation was focused on motor-reducer internal parts.

Examination and SEM/EDAX analysis of the planetary gears and pins demonstrated that the MoS₂ on the teeth was generally in good condition, although some localised patches were found where the MoS₂ was patchy. However, metallic contact was prevented by the WC coating applied to the gears.

The bores of the planets exhibited some marks where they contacted the pins and the MoS₂ appeared depleted, although the conforming contact ensured that debris was transferred and did not escape from the contact. The end faces where the gears contacted the carrier plates exhibited some wear of the MoS₂, but it was not completely removed.

The planetary gear pins exhibited some circumferential marks and wear of the MoS₂. It is clear, however, that the planetary gears and pins still have some life margin, although they are predicted to be the next components which could fail if operation could have been extended.

The examination concludes that the reason of the failure was the Rear Motor Rotor Bearing which exhibited heavy steel wear on the raceways and on the cage. Although it was subjected to the same operational conditions, the Front Motor Rotor Bearing still had some lifetime margin. Analysis using EDAX confirmed the presence of O-peaks on areas where the MoS₂ had worn, areas where it was intact and in Fe debris. However, it was not possible to determine if this O originated from moisture or O in the purged environment.

Based upon the information obtained from this analysis, the cause of failure of the Rear Motor Bearing was due to wear of the MoS₂ film lifetime applied to the bearing. Wear of the MoS₂ at the ball pockets and at the contact with the inner ring land eventually led to steel particles being released followed by bearing failure. The variability in the lifetime of this coatings together with the differences in dimensional tolerances between those cages could have led to the failure of the rear bearing much in advance of the front bearing. It is concluded that an MoS₂-coated steel cage is not ideal for long life applications and it is recommended that they should be replaced with PGM-HT cages which have considerable heritage in long-life applications and have also been used in cryogenic mechanism bearings for space. For the last 10 years CDA has used non-metallic retainers, such as PGM-HT, in its dry lube designs. The use of these cages will increase the bearing's life and eliminate the risk of generating metallic debris if the bearing's cages contact their races.

8. ACKNOWLEDGEMENTS

We would like to thank ESA, CDA and ESTL, especially Paolo Zaltron (ESA), Jameson Barlow (CDA) and Mike Anderson (ESTL) for their support and

involvement during the investigations after actuator failure.

9. REFERENCES

1. Compostizo, C., Lopez, R. & Rivera, L. (2011). GAIA M2M Pointing Mechanism Qualification. ESMATS 2011.
2. Artiagoitia, A., Compostizo, C. & Rivera, L. (2017). EUCLID M2 Mirror Mechanism. ESMATS 2017.